Original Research Article

Fundamental Acoustic Wave Generation in Crystalline Organic Conductors with Two Conducting Channels

ABSTRACT

A linear thermoelectric generation of a fundamental acoustic wave in organic conductors with two conducting channels, quasi-one dimensional (q1D) and quasi-two dimensional (q2D), is analyzed theoretically. Specifically, the case when an acoustic wave with a fundamental frequency ω is generated along the most conducting axis of the multi-band organic conductor α-(BEDT-TTF)$_2$KHg(SCN)$_4$ is considered. The magnetic field and angular dependences of the wave amplitude for two boundary conditions, isothermal and adiabatic are obtained. Findings show that the wave amplitude for the isothermal boundary is much larger than the one for the adiabatic boundary although there is a heat flux through the conductor's surface in the former. This is completely different compared to the case of a wave generated along the least conducting axis and the possible reasons behind this behavior are discussed. The angular oscillations of the fundamental wave amplitude are associated with the charge carriers motion on both the cylindrical part and quasi-planar sheets of the Fermi surface in a tilted magnetic field. The changes in the wave amplitude with the field orientation are correlated with the corresponding angular changes in the in-plane thermoelectric coefficient and thermal conductivity. Following the magnetic field behavior of both the in-plane electromagnetic and thermal skin depth we find that the wave generation and propagation in the plane of the layers are determined mainly by the thermal wave as its skin depth is thousand times larger than the one of the electromagnetic wave. It is shown that both the q1D and q2D charge carriers contribute to the observation of the effect but the group of charge carriers with a q1D energy spectrum is significantly dominant in the generation of the fundamental acoustic wave in the plane of the layers.

Keywords: Organic conductors, q1D and q2D group of charge carriers, thermoelectric effect, high-frequency fundamental acoustic wave, angular oscillations of the fundamental acoustic wave (AOFAW), magnetotransport anisotropy.

1. INTRODUCTION

Crystalline organic conductors have been among the most exciting objects in solid state physics and chemistry over the last two decades, providing a laboratory not only for studying virtually all the ground states known in condensed matter physics but also for discovering new ones. The organic conductors based on the bis(ethylenedithio)tetrath-iafulvalene molecule (BEDT-TTF, or, shorter, ET) have initially attracted attention due to the discovery of the ambient pressure superconductivity in a layered cation radical salt β-(ET)$_2$I$_3$ [1]. Further extensive efforts on the synthesis and studies of new salts of ET and its derivatives gave rise to a new generation of quasi-two-dimensional compounds [2] with properties ranging from magnetic dielectric to superconducting, depending on the chemical composition and external conditions such as temperature, pressure and magnetic field.

In organic conductors large variations in the magnetoresistance are observed as the direction of the magnetic field is varied and are referred to as angular-dependent magnetoresistance oscillations (AMRO) [3]. These effects in quasi-one-dimensional systems are known as Danner [4], Lebed [5, 6], and third angular effects [7, 8], depending on whether the magnetic field is rotated in the *ac*, *bc*, or *ab* plane, respectively. (The *a* and *c* axes are the most- and least-conducting directions, respectively). Oscillations in quasi-two-dimensional systems include the Yamaji [9] oscillations and the anomalous AMRO in the low-temperature phase (LTP) of two-band organic conductors α-(BEDT-TTF)$_2$MHg(SCN)$_4$ [M=K, Rb, Tl] [3]. The family α-(BEDT-TTF)$_2$MHg(SCN)$_4$ [M=K, Rb, Tl] are of particular interest because they have a rich phase diagram and coexisting quasi-one dimensional and

quasi-two dimensional Fermi surface (FS) [10, 11]. Metallic, superconducting, and density wave phases are possible, depending on temperature, pressure, magnetic field, and anion type. At ambient pressure, the family with M=K, Rb, Tl undergo a transition from a metal to a charge density wave (CDW) phase at a temperature T_{CDW}=8 [12], 10 [13], and 12 K [14], respectively. On passing through the "kink-field" transition at B_k=23 T (for M = K), the CDW is removed and is replaced by a metallic phase with a FS consisting of a quasi-two dimensional (q2D) hole cylinder, known as the α pocket, and a pair of quasi-one dimensional (q1D) electronic sheets [15, 16]. The low-dimensional character of the organic conductors leads to important consequences in their response to a magnetic field. In fact, numerous drastic deviations from the conventional three-dimensional behavior and even qualitatively new effects, in particular related to the field orientation, have been found in these materials (see Ref. [17]).

Generation of acoustic oscillations in solids by an electromagnetic wave can occur in a linear regime, when the frequency of the incident wave is equal to the frequency of the excited wave, and in a nonlinear regime, when the frequency of the excited elastic waves is a multiple of the frequency of the electromagnetic wave. In materials that are good conductors, both linear and nonlinear electromagnetic excitations of ultrasound occur as a result of interaction of the electromagnetic wave with the conduction electrons.

The mechanisms of linear transformation, which are responsible for the generation of high-frequency acoustic waves in conducting media at the frequency ω of an electromagnetic wave incident on the surface of the metal, are a standard subject of investigation in electromagnetic-acoustic conversion problems. The induction [18-21] and deformation force [22-27] have been studied in greatest detail as sources of linear generation of acoustic waves, i.e., fundamental wave generation with frequency ω. Apart from the induction and deformation forces, longitudinal acoustic waves at fundamental frequency can also be generated by thermoelectric forces [28-31]. In conducting media, the mechanism occurs as follows: when an electromagnetic wave with frequency ω is incident on the conductor, nonuniform temperature oscillations of the same frequency appear as a result of the thermoelectric effect. These oscillations, in turn, generate acoustic oscillations in the conductor with a frequency ω that coincides with the frequency of the incident electromagnetic wave (contactless acoustic wave generation).

The purpose of the present work is to study the magnetic field and angular dependence of the amplitude of a fundamental high-frequency acoustic wave $(\omega = 10^9\ \mathrm{Hz})$ generated through linear thermoelectric effect in the metallic phase of organic conductors with two conducting channels, quasi-one dimensional (q1D) and quasi-two dimensional (q2D). By far, this phenomenon has been considered in organic conductors with only q2D group of charge carriers [32] and in two-band organic conductors for an acoustic wave that is generated along the least conducting axis, $z-$axis [33]. The present work analyzes the generation of a high-frequency acoustic wave in two-band organic conductors along the most conducting $x-$axis. The results obtained show that the amplitude of the fundamental acoustic wave is by far larger than the one of a wave that is generated along the least conducting axis. In addition, for generation along the most conducting axis the amplitude of the fundamental wave for the isothermal boundary is always larger than the one for the adiabatic boundary although there is a heat flux through the conductor's surface in the former. We suggest that the distinct behavior of the fundamental wave for both geometries is correlated with the high magnetotransport anisotropy in these materials. The changes in the amplitude of the induced acoustic wave with the magnetic field orientation are associated with the angular dependent changes in both the in-plane thermoelectric coefficient and thermal conductivity. The period of angular oscillations of the acoustic wave generated along the layers is half the period of angular oscillations of the wave generated across the layers indicating that generation of a fundamental acoustic wave in the plane of the layers is significantly affected by the q1D charge carriers. In highly anisotropic organic conductors due to the small electron mean free-path the thermoelectric generation of high-frequency fundamental acoustic waves can be observed in a wide range of fields and angles providing possibilities for experimental studies using non-contact ultrasonic techniques. Such studies will give new insights into the unusual electronic properties of these systems.

2. LINEAR FUNDAMENTAL ACOUSTIC WAVE GENERATION: FORMULATION OF THE PROBLEM

A high-frequency fundamental acoustic wave with frequency ω is generated as a result of temperature oscillations which are induced by an electromagnetic wave with the same frequency. Here we consider a case when an electromagnetic wave $\mathbf{E} = (0, E_y, 0)$ with frequency ω is incident normally on the conductor's surface along the most conducting axis ($x-$axis), $\mathbf{k} = (k, 0, 0)$ of a multi-band organic conductor. In that case, the only nonzero component of the current density is the $y-$component, $\mathbf{j} = (0, j_y, 0)$. The fundamental wave is generated and propagating along the most conducting axis ($x-$axis), and therefore all of the quantities depend only on the $x-$component. The conductor is placed in magnetic field oriented at an angle θ from the normal to the plane of the layers, in the xz plane, $B = (B\sin\theta, 0, B\cos\theta)$. A temperature oscillating with frequency ω occurs only if the condition $\omega\tau << 1$ is satisfied, where τ is the relaxation time of the conduction electrons. We study the case of a normal skin effect when the condition $k_T l << 1$, where l is the electron mean-free path length and k_T is the thermal wave number, is fulfilled.

2.1 System of equations. Calculation of the temperature distribution $\Theta(x)$

The complete system of partial differential equations, describing the generation of longitudinal fundamental wave at frequency ω includes Maxwell's equations for the magnetic $\mathbf{B}$ and electric $\mathbf{E}$ field, the kinetic equation for the nonequilibrium correction Ψ to the electron distribution function $f_0(\varepsilon)$, and the equations of heat conduction and the theory of elasticity for ionic displacement $\mathbf{U} = (U_\omega, 0, 0)$:

$$\operatorname{curl}\mathbf{B} = \mu_0\mathbf{j}; \quad \operatorname{curl}\mathbf{E} = -\frac{\partial\mathbf{B}}{\partial t}, \tag{2.1}$$

$$\left(\frac{\partial}{\partial t} + \mathbf{v}\nabla + e\left[\mathbf{v}\mathbf{B}\right]\frac{\partial}{\partial\mathbf{p}} + \frac{1}{\tau}\right)\Psi = -e\,\mathbf{v}\mathbf{E} + \frac{\varepsilon-\mu}{k_B T}\mathbf{v}\nabla T, \tag{2.2}$$

$$C\frac{\partial\Theta}{\partial t} + \operatorname{div}\mathbf{Q} = 0, \; Q_i = k_B T\alpha_{ik}\frac{\partial j_k}{\partial x_k} - \kappa_{ik}\frac{\partial\Theta}{\partial x_k}, \tag{2.3}$$

$$\rho\frac{\partial^2 U_i}{\partial t^2} - \lambda_{iklm}\frac{\partial U_{lm}}{\partial x_k} = -\rho s^2\beta\delta_{ik}\frac{\partial\Theta}{\partial x_k}. \tag{2.4}$$

Here μ_0 is the magnetic permeability of the vacuum, $\mathbf{v}$ and $\mathbf{p}$ are the electron velocity and momentum, e is the electron charge, $\mathbf{Q}$ is the heat flux, Θ is the high-frequency addition to the mean temperature T of the crystal, μ is the chemical potential, C is the volumetric heat capacity, k_B is the Boltzmann constant, α_{ik} is the thermoelectric coefficient, κ_{ik} is the thermal conductivity, ρ is the density of the crystal, δ_{ik} is the Kronecker delta, s is the fundamental acoustic wave velocity and β is the volumetric expansion coefficient. $U_{lm} = (\partial U_l/\partial x_m + \partial U_m/\partial x_l)/2$ is the deformation tensor and λ_{iklm} are components of the elastic tensor of the crystal. The subscripts in U and x describe the wave polarization and direction of wave propagation, respectively. The wave is taken to be monochromatic, so the differentiation with respect to the time variable is equivalent to multiplication by $(-i\omega)$.

For the given geometry the above system of equations (2.1-2.4) takes the following form

$$\frac{\partial B_z}{\partial x} = \mu_0 j_y; \quad \frac{\partial E_y}{\partial x} = i\omega B_z, \tag{2.5}$$

$$\left(\frac{\partial}{\partial t_B} + \frac{1}{\tau}\right)\Psi = v_y\left(eE_y + \frac{\varepsilon - \mu}{k_B T}\frac{\partial T}{\partial x}\right), \tag{2.6}$$

$$-i\omega C\Theta - \kappa_{xx}\frac{\partial^2 \Theta}{\partial x^2} = -k_B T\alpha_{xy}\frac{\partial j_y}{\partial x}, \tag{2.7}$$

$$\frac{\partial^2 U_\omega}{\partial x^2} + q^2 U_\omega = \beta\frac{\partial \Theta}{\partial x}. \tag{2.8}$$

Here t_B is the time of motion of the conduction electrons in a magnetic field under the influence of the Lorentz force with a period $T_p = 2\pi/\omega_c$ and cyclotron frequency $\omega_c = eB\cos\theta/m^*$. κ_{xx} and α_{xy} are the in-plane thermal conductivity and thermoelectric coefficient and $q = \omega/s$ is the acoustic wave vector.

The above system of equations must be supplemented with the corresponding boundary conditions for the temperature distribution and fundamental acoustic wave amplitude at the conductor's surface. Two types of boundary are considered, isothermal and adiabatic for which the boundary conditions are defined as follows:

$$\Theta|_{x=0} = 0, \qquad \kappa_{xx}\frac{\partial \Theta}{\partial x}|_{x=0} = 0, \tag{2.9}$$

$$U_\omega|_{x=0} = 0, \quad \frac{\partial U_\omega}{\partial x}|_{x=0} = -\beta\frac{\partial \Theta}{\partial x}|_{x=0}. \tag{2.10}$$

By using Maxwell's equations one obtains the following expression for the current density

$$j_y = \frac{ik_E^2}{\omega\mu_0} Exp[i(k_E x - \omega t)], \tag{2.11}$$

where $k_E = (1+i)/\delta_E$ and $\delta_E = (2\rho_{yy}/\omega\mu_0)^{1/2}$ are the wave vector and skin depth of the electromagnetic field, respectively.

Substituting eq. (2.11) into the heat conduction equation (2.7) we obtain the following partial differential equation for the temperature distribution within the conductor

$$\frac{\partial^2 \Theta}{\partial x^2} + k_T^2\Theta = \frac{k_E^3 k_B T\alpha_{xy}}{\kappa_{xx}\omega\mu_0} Exp\ [ik_E x], \tag{2.12}$$

where $k_T = (1+i)/\delta_T$ and $\delta_T = (2\kappa_{xx}/\omega C)^{1/2}$ are the wave vector and skin depth of the thermal field under the conditions of a normal skin effect.

Crucial part in further theoretical analysis is to obtain the solutions of the eq. (2.12) and substitute them in the eq. (2.8) for the amplitude of the generated fundamental acoustic wave to be determined. The linear acoustic wave generation due to thermoelectric effect, i.e., generation of an acoustic wave with fundamental frequency ω, can be observed only when the coupling between the electromagnetic and temperature oscillations is weak, i.e., when the parameter $a = k_B T(\alpha_{xy}^2/\rho_{yy}\kappa_{xx})$ that determines

the coupling between the two oscillations is much smaller than 1, $a \ll 1$. In that case, the temperature distribution that results from the oscillations of the current density $\mathbf{j}$ can be determined.

Using the boundary conditions for the temperature (eq. (2.9)) the following solution for the temperature distribution within the conductor is obtained

$$\Theta(x) = \frac{k_E k_B T \alpha_{xy}}{\kappa_{xx} \omega \mu_0} \frac{1}{k_T^2 - k_E^2} \left(Exp\,[ik_E x] - b\, Exp\,[ik_T x] \right), \tag{2.13}$$

where b is 1 for an isothermal boundary condition, and k_T / k_E for an adiabatic boundary condition.

2.2 Calculation of the fundamental acoustic wave amplitude $U_\omega(x)$

By substituting the obtained expression for the temperature distribution $\Theta(x)$ (eq. (2.13)) and using the boundary conditions for the wave amplitude (eq. (2.10)) into the equation of the theory of elasticity (2.8), calculations yield the following expressions for the complex amplitude of the fundamental acoustic wave excited by the temperature oscillations for both the isothermal and adiabatic boundary:

$$U_\omega^i(x) = i \frac{k_B T \beta \alpha_{xy} \kappa_{xx}}{C \omega (\rho_{yy} \omega \mu_0)^{1/2}} \frac{1}{(\rho_{yy} / \omega \mu_0)^{1/2} + (\kappa_{xx} / \omega C)^{1/2}} \tag{2.14}$$

$$U_\omega^a(x) = (1-i) \frac{\sqrt{2\mu_0} k_B T \beta \alpha_{xy} \kappa_{xx}}{q\,(\rho_{yy} \omega)^{1/2}} \frac{1}{\rho_{yy} C + (\rho_{yy} \kappa_{xx} C \mu_0)^{1/2}} \tag{2.15}$$

The components of the conductivity tensor which relate the current density to the electric field can be calculated by using the Boltzmann transport equation for the charge carrier distribution function, based on the tight binding approximation band structure within the single relaxation time approximation τ (eq. (2.6)) [34]. The components of the electrical conductivity and thermoelectric tensor are determined as follows

$$\sigma_{ij} = \frac{2e^3 B}{(2\pi\hbar)^3} \int \frac{\partial f_0}{\partial \varepsilon} d\varepsilon \int dp_B \int_0^{T_p} dt v_i(t) \Psi_j . \tag{2.16}$$

$$\alpha_{ij} = \frac{2e^3 B}{(2\pi\hbar)^3} \int \frac{\varepsilon - \mu}{k_B T} \frac{\partial f_0}{\partial \varepsilon} d\varepsilon \int dp_B \int_0^{T_p} dt v_i(t) \Psi_j . \tag{2.17}$$

Here $\hbar$ is the Planck's constant divided by 2π, $p_B = p_x \sin\theta + p_z \cos\theta = \text{const}$ is the momentum projection in the magnetic field direction.

We shall assume that the velocities $\pm \mathbf{v}_1$ of the electrons belonging to the plane sheets of the FS, i.e., the q1D group of charge carriers are predominantly oriented in a direction determined by an angle ϕ so that their velocities are $v_{1x} = \pm v_1 \cos\phi$, $v_{1y} = \pm v_1 \sin\phi$ and the dispersion law for the charge carriers belonging to a weakly warped FS cylinder has the form

$$\varepsilon(p) = \frac{p_x^2 + p_y^2}{2m^*} + \eta \frac{v_F \hbar}{c} \cos\left(\frac{c p_z}{\hbar}\right) \tag{2.18}$$

where m^* is the electron cyclotron effective mass, η is the quasi-two dimensionality parameter, v_F is the characteristic Fermi velocity of the electrons along the layers and c is the lattice constant.

We shall assume that the angle of deviation of the magnetic field from the direction normal to the layers is not too close to $\pi/2$ so that all orbits of electrons with a quadratic dispersion law are closed and do not contain self-intersections. The components of the conductor's kinetic coefficients σ_{ij} are a sum of the contributions of quasi-one dimensional q1D and quasi-two dimensional q2D charge carriers, which are calculated using the eq. (2.16). Specifically, the following expressions are obtained for the components of the conductivity tensor

$$\sigma_{xx} = \sigma_{xx}^{\mathrm{q2D}} + \sigma_{xx}^{\mathrm{q1D}} = \frac{\gamma^2 \sigma_2}{B^2 \cos^2\theta}(1 - \sigma_{zz}^{\mathrm{q2D}} \tan^2\theta) + \sigma_1 \cos^2\phi, \tag{2.19}$$

$$\sigma_{yy} = \sigma_{yy}^{\mathrm{q2D}} + \sigma_{yy}^{\mathrm{q1D}} = \left(\frac{\gamma^2 \sigma_2}{B^2 \cos^2\theta} + \sigma_{zz}^{\mathrm{q2D}} \tan^2\theta\right) + \sigma_1 \sin^2\phi, \tag{2.20}$$

$$\sigma_{xy} = \sigma_{xy}^{\mathrm{q2D}} + \sigma_{xy}^{\mathrm{q1D}} = \frac{\gamma \sigma_2}{B\cos\theta}(1 - \sigma_{zz}^{\mathrm{q2D}} \tan^2\theta) + \sigma_1 \cos\phi \sin\phi, \tag{2.21}$$

$$\sigma_{zz}^{\mathrm{q2D}} = \sigma_2 \cos\theta J_0^2\left(\frac{cD_p \tan\theta}{\hbar}\right). \tag{2.22}$$

Here σ_1 and σ_2 are the contributions to the electrical conductivity along the layers with $\mathbf{B} = 0$ of q1D and q2D group of charge carriers, $D_p = 2p_F$ is the averaged diameter of the FS along the p_x- axis, J_0 is the zeroth order Bessel function and $\gamma = m^*/e\tau.$

In $\tau-$approximation, it is suffcient to calculate the components of the electrical conductivity tensor and the rest of the kinetic and thermoelectric coeffcients, describing the heat flux and thermoelectric effects, are obtained as follows

$$\rho_{yy} = \sigma_{yy}^{-1} = 1 + \frac{\sigma_1}{\sigma_2}\frac{B^2 \cos^2\theta \cos^2\phi}{\gamma^2}, \tag{2.23}$$

$$\begin{aligned} \alpha_{xy} &= \frac{\pi^2 k_B T}{3e^2}\frac{\partial \sigma_{xy}}{\partial \varepsilon}\Big|_{\varepsilon=\mu} = \\ &= \frac{\pi^2 k_B T}{3e^2 \mu}\left(\frac{\gamma \sigma_2}{B\cos\theta} + \sigma_1 \cos\phi \sin\phi\right) - \frac{\pi^2 k_B T}{3e^2}\frac{\gamma \sigma_2}{B\cos\theta}\alpha_{zz} \tan^2\theta, \end{aligned} \tag{2.24}$$

$$\alpha_{zz} = \frac{\pi^2 k_B T}{3e^2}\frac{\partial \sigma_{zz}^{\mathrm{q2D}}}{\partial \varepsilon}\Big|_{\varepsilon=\mu} = \frac{\pi^2 k_B T}{3e^2}\frac{\sigma_2}{\mu}\left(4\sin\theta J_0\left(\frac{cD_p \tan\theta}{\hbar}\right) J_1\left(\frac{cD_p \tan\theta}{\hbar}\right)\right), \tag{2.25}$$

$$\kappa_{xx} = \frac{\pi^2 k_B^2 T}{3e^2}\sigma_{xx}. \tag{2.26}$$

3. RESULTS AND DISCUSSION

3.1 Angular oscillations of the fundamental acoustic wave (AOFAW)

The amplitude of the generated acoustic wave with fundamental frequency due to thermoelectric effect is a function of the frequency of applied electric current ω, the magnetic field B, the angle between the normal to the layers and the magnetic field θ as well as of the kinetic and thermoelectric characteristics of the conductor: electrical and thermal conductivity as well as the thermoelectric coefficient. For the multi-band organic conductor α–(BEDT-TTF)$_2$KHg(SCN)$_4$ the cyclotron mass

extracted from data on magnetic quantum oscillations is $m^* = 3.5m_e$ (m_e is the free electron mass) and the relaxation time is of the order of $\tau = 2\times10^{-12}$ s [17]. We assume that the q1D plane sheets and q2D FS cylinder are not strongly corrugated and the quasi-two dimensionality parameter is of order $\eta = 0.01$.

The angular oscillations are characteristic of the kinetic and thermoelectric coefficients of layered organic conductors and do not occur in isotropic metals. Since the amplitude of the acoustic wave is determined by both the kinetic and thermoelectric coefficients angular oscillations of the amplitude of the generated fundamental acoustic wave are expected to emerging when a constant magnetic field is turned from the direction normal to conducting layers toward the plane of the layers. The angular oscillations are associated with the charge carriers motion on both the cylindrical part and quasi-planar sheets of the FS in a tilted magnetic field. The existence of points at which the interaction with the wave is most effective on different trajectories leads to a resonant dependence of the acoustic wave amplitude on magnetic field B and the angle between the normal to the layers and magnetic field θ. Resonant oscillations of the amplitude U_ω on the tangent of the angle between the normal to the layers and magnetic field for both the isothermal and adiabatic boundary at $T = 30$ K, $B = 0.6$ T and $\phi = 85^0$ are shown in Fig. 1. The amplitude $U_\omega(\tan\theta)$ exhibits giant oscillations as the value at the peaks is much larger (about two times larger) than the one at the minimum. The angular oscillations of the fundamental wave are observed when the field is tilted close to the plane of the layers, i.e., for $\tan\theta > 7$ ($\theta > 82^0$) as expected since we consider a wave generation in the plane of the layers. The amplitude of the wave increases very fast with tilting the angle towards the plane of the layers, i.e., towards the $x-$axis, in proportion to $(\tan\theta)^4$ since $U_\omega^{i,a} \sim \alpha_{xy}\kappa_{xx} \sim (\tan\theta)^4$. In addition, with tilting the field from the $z-$axis, the drift of charge carriers along the $z-$axis, $\bar{v}_z$, decreases but the drift along the $x-$axis, $\bar{v}_x = \bar{v}_z \tan\theta$, is rather large at angles close to $\theta = 90^0$.

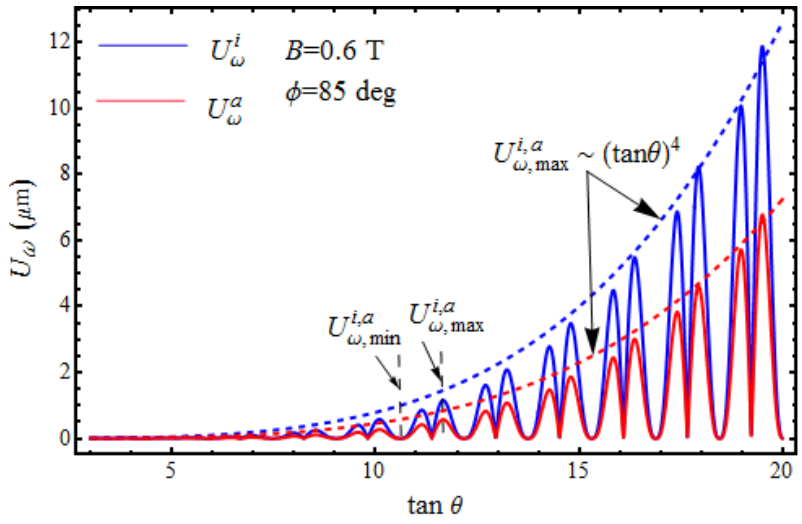

Fig. 1. Angular oscillations of the fundamental acoustic wave amplitude U_ω in the plane of the layers for isothermal (blue curve) and adiabatic (red curve) boundary at $T = 30$ K, $\eta = 0.01$, $B = 0.6$ T and $\phi = 85^0$. The dashed lines indicate the positions of the maxima $U_{\omega,\max}^{i,a}$ and minima $U_{\omega,\min}^{i,a}$ of the wave amplitude for both boundaries.

An important feature to emphasize is that the amplitude of the fundamental wave for the isothermal boundary is larger than the one for the adiabatic boundary although there is a heat flux through the conductor's surface in the former. Our suggestion is that the reason for this behavior is the larger adiabatic resistivity in the case of a fundamental acoustic wave generated along the layers. In fact,

when the thermoelectric coefficient is not too small (as in the case of the in-plane thermoelectric coefficient α_{xy}), a distinction must be made between isothermal ρ_i and adiabatic ρ_a resistivities, i.e., $\rho^a = \rho^i(1 + k_B T \alpha_{xy}^2 / \rho^i \kappa_{xx})$. Due to the larger resistivity in the adiabatic case the fundamental wave generated under the conditions of adiabatic boundary is more strongly attenuated than in the isothermal case.

The minima in the $U_\omega(\tan\theta)$ dependence correspond to the zero amplitude of the fundamental acoustic wave and their positions coincide with the positions of the zeros in the angular dependence of the in-plane thermoelectric coefficient $\alpha_{xy}(\tan\theta)$ as shown in Fig. 2. The in-plane thermal conductivity is negative in the whole range of angles which indicates that the in-plane conductivity is also negative as $\kappa_{xx} \sim \sigma_{xx}$ implying that the dominant carriers in the fundamental wave generation are the electron-like carriers, i.e., the q1D group of charge carriers. This is expected as in the multi-band organic conductor α–(BEDT-TTF)$_2$KHg(SCN)$_4$ the q1D charge carriers drift mainly along the $x-$axis and this is the direction along which the wave is generated.

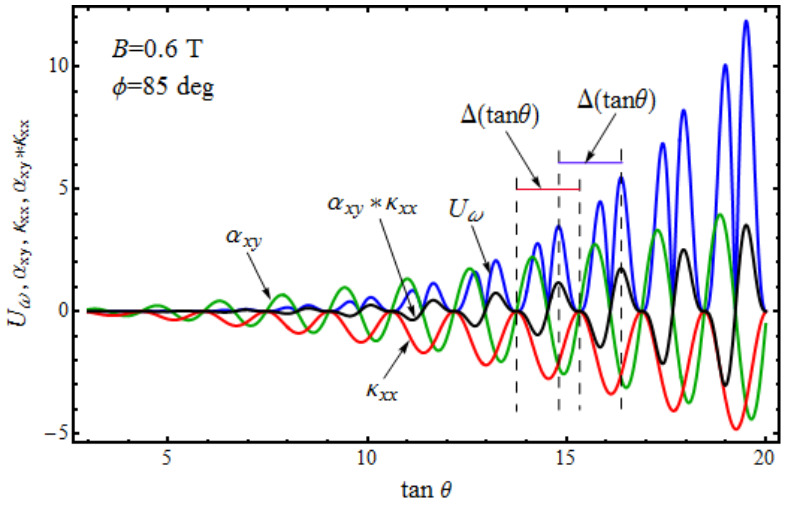

Fig. 2. Angular positions of the fundamental acoustic wave amplitude U_ω for isothermal boundary (blue curve), in-plane thermoelectric coefficient α_{xy} (green curve), in-plane thermal conductivity κ_{xx} (red curve) and the term $\alpha_{xy}\kappa_{xx}$ (black curve) at $T = 30\,\mathrm{K}$, $\eta = 0.01$, $B = 0.6\,\mathrm{T}$ and $\phi = 85^0$. The dashed lines indicate the positions of the peaks of the amplitude U_ω and in-plane thermal conductivity κ_{xx}.

The in-plane conductivity σ_{xx} is determined by the interlayer conductivity σ_{zz} (eq. 2.19) and the direction of the q1D charge carriers ϕ in the plane of the layers. When $\tan\theta >> 1$ electrons may execute many orbits before dephasing, resulting in the resonance. In that case, the first term in eq. (2.19) for the in-plane conductivity σ_{xx} is dominant. It follows from eq. 2.(19) that when $cD_p \tan\theta/\hbar$ equals a zero of the zeroth-order Bessel function, then at that angle the electrical conductivity along the less conducting axis, $\sigma_{zz}(\theta)$, will be negligible and consequently the in-plane conductivity $\sigma_{xx}(\theta)$ vanishes at the same angle. These are known as Yamaji angles [9]. If $cD_p \tan\theta/\hbar >> 1$, then the zeros in $\sigma_{xx}(\theta)$ and $\kappa_{xx}(\theta)$ occur at angles $\theta = \theta_n^{\min}$, given by $cD_p \tan\theta_n^{\min}/\hbar = \pi(n - 1/4)$, $n = 0, 1, 2, 3...$ For $\sigma_{xx}(\theta)$ and $\kappa_{xx}(\theta)$ to be a maximum it should be $\theta = \theta_n^{\max}$, where $cD_p \tan\theta_n^{\max}/\hbar = \pi(n + 1/4)$. The positions of the peaks in the $U_\omega(\tan\theta)$ dependence do not coincide with the position of the maxima of the thermal conductivity as seen in Fig. 2. Instead, their

positions coincide with the positions of the extremes of the term $\alpha_{xy}\kappa_{xx}(\tan\theta)$ as expected since this term is the one that determines the field and angular behavior of the wave amplitude. The term $\alpha_{xy}\kappa_{xx}$ shows resonant like behavior which is existence of two close to each other extremes, with sign change at angles that correspond to the angles where the in-plane thermal conductivity has maximum or minimum, $\theta=\theta_n^{\max},\theta_n^{\min}$. This, in turn, reflects as appearance of two close maxima in the $U_\omega(\tan\theta)$ dependence. In the vicinity of angles $\theta=\theta_n^{\max}$, the drift velocity $\bar{v}_x$ of charge carriers along the acoustic wavevector coincides with the velocity s of the acoustic wave, and their interaction with the wave is most effective. As a result, at these angles the amplitude is the largest (especially this trend is apparent for $\tan\theta>>1$) and $U_\omega(\tan\theta)$ exhibits giant oscillations. The narrow peaks that appear in the $U_\omega(\tan\theta)$ dependence repeat with a period $\Delta(\tan\theta)=2\pi\hbar/cD_p$ which is the same as the period of oscillations of the in-plane thermal conductivity $\kappa_{xx}(\tan\theta)$ as evident from Fig. 2. This is different from the case of an organic conductor with only q2D charge carriers where the period of the acoustic wave amplitude generated along the least conducting axis is half the period of angular oscillations of the inverse interlayer conductivity $\kappa_{zz}^{-1}(\tan\theta)$ [32]. This indicates that the presence of group of charge carriers with a q1D energy spectrum significantly affects the generation of the fundamental acoustic wave in the plane of the layers.

3.2 Magnetic field dependence of the fundamental acoustic wave amplitude

Fig. 3 shows the magnetic field dependence of the amplitude of the generated fundamental acoustic wave in α–(BEDT-TTF)$_2$KHg(SCN)$_4$ for both the isothermal and adiabatic boundary at $\theta=85^0$ and $\phi=89^0$.

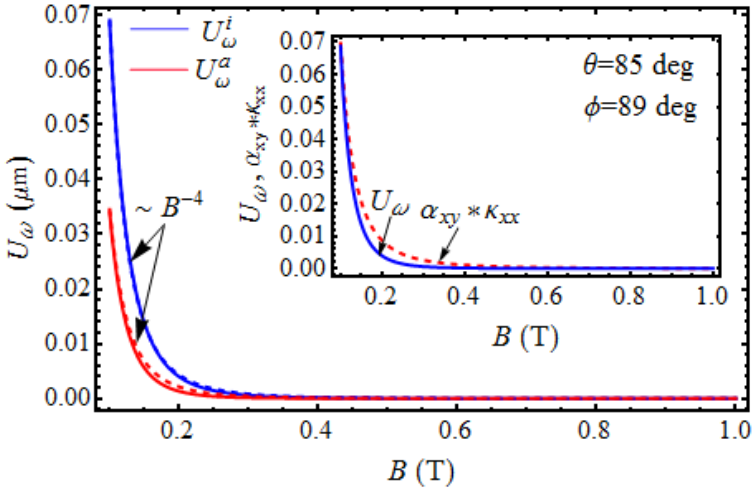

Fig. 3. Magnetic field dependence of the fundamental acoustic wave amplitude $U_\omega(B)$ for isothermal (blue curve) and adiabatic (red curve) boundary at $T=30$ K, $\eta=0.01$, $\theta=85^0$ and $\phi=89^0$. The dashed lines indicate the B^{-4} field dependence of the wave amplitude for both boundaries. The inset shows the magnetic field dependence of $\alpha_{xy}\kappa_{xx}$ (red dashed curve) compared to $U_\omega(B)$ (blue solid curve). $\alpha_{xy}\kappa_{xx}$ is following the same B^{-4} field dependence as the amplitude $U_\omega(B)$.

The fundamental wave generation starts at zero field and the amplitude decreases with increasing field for both boundaries. It is obvious that the in-plane generated fundamental wave is strongly attenuated with increasing field and its amplitude decreases in proportion to B^{-4}. The observed field

dependence originates from the magnetic field behavior of the term $\alpha_{xy}\kappa_{xx}$ (that determines the amplitude $U_{\omega}^{i,a}$) which is also following the B^{-4} dependence as seen from the inset in Fig. 3. This is completely different form the case of an acoustic wave generated along the least conducting axis, i.e., the interlayer fundamental wave previously considered in [33] where the wave amplitude is decreasing with increasing field approximately as B^{-1}. It is instructive to discuss here presented results in the context of previous studies on the interlayer acoustic wave generation. We first note that the amplitude of the in-plane wave is much larger than the one of the interlayer fundamental wave of order of 10^{-3}. This is conditioned by the high magnetotransport anisotropy, i.e., by the high conductivity anisotropy ratio of the interlayer and in-plane conductivity in α–(BEDT-TTF)$_2$KHg(SCN)$_4$. It follows that the larger amplitude of the in-plane acoustic wave is due to the large in-plane electrical conductivity and consequently due to the large number of charge carriers (q1D and q2D) included in the process of the thermoelectric acoustic wave generation. Another difference between the two geometries is that the isothermal wave amplitude exceeds the adiabatic in a whole range of fields. This implies that when performing experiments on in-plane acoustic wave generation the isothermal boundary is preferable in the whole range of fields. For the interlayer wave generation the preference of one type of a boundary over another depends on the magnetic field strength. In addition, the in-plane acoustic wave is more strongly attenuated with increasing field (despite the much larger amplitude) than the interlayer acoustic wave. This is evident from the stronger field dependence (B^{-4}) in the former compared to the B^{-1} dependence in the latter [33] and is correlated with the magnetic field behavior of the thermal skin depth as well as the corresponding contributions from the q1D and q2D charge carriers as discussed below.

3.3 In-plane electromagnetic and thermal skin depth

Fig. 4 shows the magnetic field dependence of the total in-plane electromagnetic and thermal skin depth as well as the corresponding contributions from the q1D and q2D charge carriers. The total electromagnetic skin depth is linear in field as it is the one for the q2D carriers but is field independent for the q1D carriers. On the other hand, the total thermal skin depth is decreasing with increasing field as it is one for the q2D carriers and is field independent for the q1D carriers as in the case of the electromagnetic skin depth. The field independence of both skin depths for the q1D carriers follows from the field independence of the in-plane electrical conductivities for the q1D carriers $\sigma_{xy}^{\mathrm{q1D}} = \sigma_1 \cos\phi \sin\phi$ and $\sigma_{xx}^{\mathrm{q1D}} = \sigma_1 \cos^2\phi$ that determine the electromagnetic and thermal skin depth, respectively.

Following the changes in skin depths with field allows to distinguish if the wave generation is deter mined by the thermal or electrodynamic characteristics of the conductor. As evident from Fig. 4 the thermal skin depth exceeds by far the electromagnetic one (it is about 20 times larger) indicating that the fundamental wave generated in the plane of the layers is mainly transmitted by the thermal waves. Our suggestion is that in the case of linear wave generation due to the weak coupling between electromagnetic and temperature oscillations the thermal skin depth is always larger than the electromagnetic one and the fundamental wave is transmitted mainly by the thermal wave that dissipates at distance $\sim\delta_T$. We find that the thermal skin depth for the q1D charge carriers is larger than the one for the q2D charge carriers (except for very low fields $B \leq 0.05\ \mathrm{T}$) corroborating above mentioned that both the q1D and q2D charge carriers contribute to the observation of the effect but the q1D charge carriers are the dominant carriers in generation and propagation of a fundamental acoustic wave along the most conducting axis in α–(BEDT-TTF)$_2$KHg(SCN)$_4$.

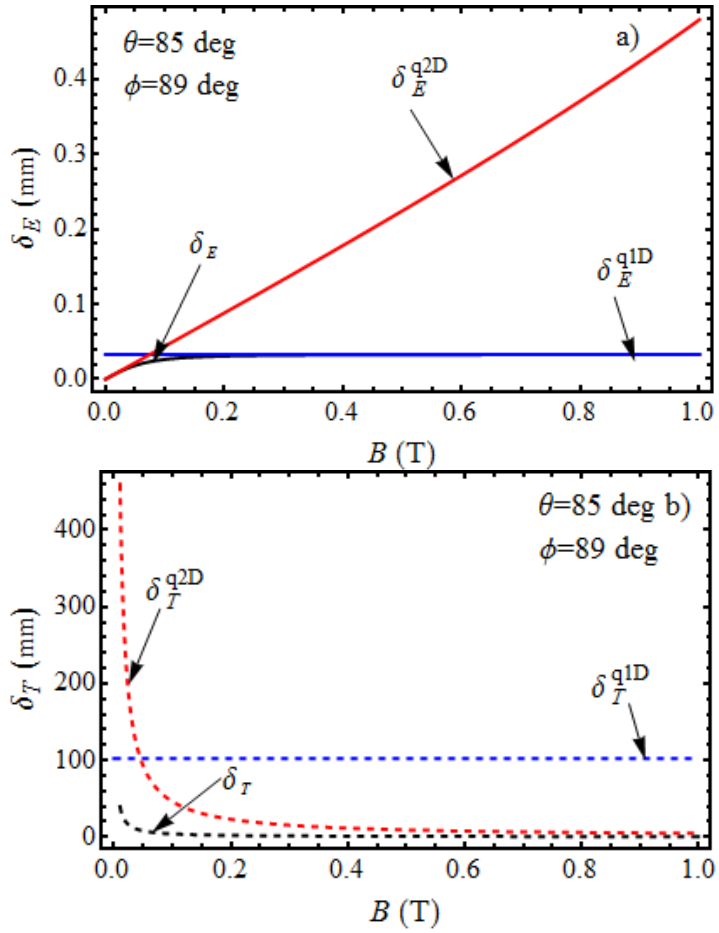

Fig. 4. Magnetic field dependence of the total in-plane a) electromagnetic and b) thermal skin depth (black curves) and the corresponding contributions from the q1D (blue curves) and q2D charge carriers (red curves) at $T = 30$ K, $\eta = 0.01$, $\theta = 85^0$ and $\phi = 89^0$.

The generation of fundamental waves is constraint by the condition $\omega\tau << 1$. In the organic conductor α–(BEDT-TTF)$_2$KHg(SCN)$_4$ this condition is always fulfilled, even at high frequencies $(\omega = 10^9$ Hz) as the relaxation time of charge carriers τ is very small $(\tau = 2\times10^{-12}$ s). In addition, for the generation of waves to be the most effective the condition $l\delta_T << 1$ must be satisfied. A Fermi velocity of $v_F = 6.5\times10^4$ m/s [35] gives an electron mean free-path of order $l = 13\times10^{-8}$ m. We have obtained from Fig. 4 the following values for the electromagnetic and thermal skin depth at $B = 0.6$ T, $\delta_E = 0.03$ mm and $\delta_T = 0.6$ mm, respectively. It is evident that the electron mean free-path l is much smaller than both skin depths providing the fundamental wave generation to be studied in detail experimentally that will give new insights into the complex electronic properties of these systems.

4. CONCLUSION

The linear generation of high-frequency acoustic waves $(\omega = 10^9$ Hz) in layered organic conductors with two groups of charge carriers, q1D and q2D, due to thermoelectric effect is considered. Only a fundamental wave is generated due to the thermoelectric stresses caused by the non-uniform temperature oscillations and its amplitude is analyzed as a function of the magnetic field B, the angle θ between the normal to the layers and the magnetic field as well as of the conductor's thermoelectric characteristics. Specifically, the parameter values for the organic conductor α–(BEDT-

TTF)$_2$KHg(SCN)4 are used to obtain the fundamental wave amplitude U_ω at $T = 30$ K and for not strongly warped open plane sheets and closed cylindrical FS. We find that the oscillatory dependence of the fundamental amplitude is determined mainly by the angular oscillations of both the in-plane thermoelectric coefficient thermal conductivity, i.e., by the angular behavior of the term $\alpha_{xy}\kappa_{xx}$ and are associated with the periodic charge carriers motion on both the cylindrical part and quasi-planar sheets of the FS in a tilted magnetic field. At angles where $U_\omega(\tan\theta)$ is maximum, the average drift velocity of charge carriers along the wave vector coincides with the wave velocity s. Therefore narrow peaks appear in the angular dependence $U_\omega(\tan\theta)$ that correspond to the most effective interaction of the charge carriers with the wave. It has been shown that the positions of the peaks of the fundamental wave angular oscillations are shifted from those of the in-plane thermal conductivity and the positions of the peaks in the $U_\omega(\tan\theta)$ dependence coincide with the positions of the extremes of the term $\alpha_{xy}\kappa_{xx}(\tan\theta)$. It is important to note that for a fundamental acoustic wave generated in the plane of the layers in organic conductors with two conducting channels the period of angular oscillations is larger compared to the one of a wave generated along the normal to the layers in organic conductors with only q2Dgroup of charge carriers.

As regards the magnetic field behavior of the wave amplitude we find that the in-plane generated fundamental wave is strongly attenuated with increasing field and its amplitude decreases in proportion to B^{-4}. The observed field dependence originates from the magnetic field behavior of the term $\alpha_{xy}\kappa_{xx}$. Comparison of the magnetic field dependence of the in-plane and interlayer generated fundamental wave shows that both waves exhibit different field dependence, B^{-4} in the former and B^{-1} in the latter. We find that the thermal skin depth is larger than the electromagnetic one and the fundamental wave is transmitted mainly by the thermal wave that dissipates at distance $\sim\delta_T$. Both the q1D and q2D charge carriers contribute to the observation of the effect but the q1D charge carriers are the dominant carriers in generation and propagation of a fundamental acoustic wave along the most conducting axis ($x-$ axis) in the multi-band organic conductor α–(BEDT-TTF)$_2$KHg(SCN)$_4$.

REFERENCES

1. Yagubskii EB, Shchegolev IF, Laukhin VN, Kononovich PA, Kartsovnik MV, Zvarykina AV et al. Normal-pressure superconductivity in an organic metal (BEDT-TTF)$_2I_3$ [bis (ethylene dithiolo) tetrathiof ulvalene triiodide]. JETP Lett. 1984;39(1):12.
2. Williams JM, Ferraro JR, Thorn RJ, Carlson K, Geiser U, Wang HH et al. Organic Superconductors: Synthesis, Structure, Properties and Theory. Prentice Hall: Englewood, Cliffs, NJ: 1992.
3. Wosnitza J. Fermi Surfaces of Low Dimensional Organic Metals and Superconductors. 1st ed. Springer: Berlin; 1996.
4. Danner KG, Chaikin PM. Non-Fermi-Liquid Behavior in Transport in (TMTSF)$_2$PF$_6$. Phys Rev Lett. 1995;75: 4690.
5. Chashechkina EI, Chaikin PM. Magic angles and the ground states in (TMTSF)$_2$PF$_6$. Phys Rev Lett. 1998;80: 2181.
6. Osada T, Kagoshima S, Miura N. Resonance effect in magnetotransport anisotropy of quasi-one-dimensional conductors. Phys Rev B. 1992;46: 1812.
7. Osada T, Kagoshima S, Miura N. Resonance effect in magnetotransport anisotropy of quasi-one-dimensional conductors. Phys Rev Lett. 1996;77: 5261.
8. Lebed AG, Bagmet NN. Nonanalytical magnetoresistance, the third angular effect, and a method to investigate Fermi surfaces in quasi-two-dimensional conductors. Phys Rev B. 1997;55: 8654.
9. Yamaji K. On the angle dependence of the magnetoresistance in quasi-two-dimensional organic superconductors. J Phys Soc Jpn. 1989;58:1520.
10. Sasaki T, Toyota N, Tokumoto M, Kinoshita N, Anzai N. Transport properties of organic conductor (BEDT-TTF)$_2$KHg(SCN)$_4$: I. Resistance and magnetoresistance anomaly. Solid State Commun. 1990;75:93.
11. Kinoshita N, Tokumoto M, Anzai N. Electron Spin Resonance and Electric Resistance Anomalyof (BEDT-TTF)$_2$RbHg(SCN)$_4$. J Phys Soc Jpn. 1991;60:2131.

12. Kusch ND, Buravov LV, Kartsovnik MV, Laukhin VN, Pesotskii SI, Shibaeva RP et al. Resistance and magnetoresistance anomaly in a new stable organic metal $(ET)_2TlHg(SCN)_4$. Synth Met. 1992;46:271.
13. Mori H, Tanaka S, Oshima M, Saito G, Mori T, Murayama Y, Inokuchi H. Crystal and Electronic Structures of $(BEDT–TTF)_2[MHg(SCN)_4](M=K$ and $NH_4)$. Bull Chem Soc Jpn. 1990;63:2183.
14. Ducasse L, Fritsch A. Effect of basis set on the band structure and Fermi surface of BEDT-TTF-based organic conductors. Solid State Comm. 1994;91:201.
15. Qualls JS, Balicas L, Brooks JS, Harrison N, Montgomery LK, Tokumoto M. Competition between Pauli and orbital effects in a charge-density-wave system. Phys Rev B. 2000;62:10008.
16. Proust C, Audouard A, Kovalev A, Vignolles D, Kartsovnik M, Brossard L et al. Quantum oscillations and phase diagram of α–$(BEDT–TTF)_2TlHg(SCN)_4$. Phys Rev B. 2000;62:2388.
17. Kartsovnik MV. High Magnetic Fields: A Tool for Studying Electronic Properties of Layered Organic Metals. Chem Rev. 2004;104:5737.
18. Kontorovich VM, Glushyuk AM. Transformation of sound and electromagnetic waves at the boundary of a conductor in a magnetic field. JETP. 1962;14(4):852.
19. Kravchenko VYa. Electromagnetic excitation of sound in a metallic plate. JETP. 1968;27(5):801.
20. V. L. Fal'ko VL. Electromagnetic generation of sound in a metal plate in a perpendicular magnetic field. JETP. 1983;58(1):175.
21. Vasil'ev AN, Gaidukov YuP. Electromagnetic excitation of sound in metals. Soviet Physics Uspekhi. 1983;26(11):952.
22. Turner G, Thomas RL, Hsu D. Electromagnetic generation of ultrasonic shear waves in potassium. Phys Rev B. 1971;3:3097.
23. Wallace WD, Gaerttner MR, Maxfield BW. Low-temperature electromagnetic generation of ultrasound in potassium. Phys Rev Lett. 1971;27:995.
24. Chimenti DE, Kukkonen CA, Maxfield BW. Nonlocal electromagnetic generation and detection of ultrasound in potassium. Phys Rev B. 1974;10:3228.
25. Chimenti DE. Nonlocal electromagnetic generation of acoustic waves in aluminum films. Phys Rev B. 1976;13:4245.
26. Banik NC, Overhauser AW. Electromagnetic generation of ultrasound in metals. Phys Rev B. 1977;16:3379.
27. Kartheuser E, Rodriguez S. Deformation potentials and the electron-phonon interaction in metals. Phys Rev B. 1986;33:772.
28. Kaganov MI, Tsukernik VM. Effect of thermoelectric forces on the skin effect in a metal. JETP. 1959;8:327.
29. Kaganov MI. Thermoelectric mechanism of electromagnetic-acoustic transformation. JETP. 1990;71:1028.
30. Kaganov MI, Maallavi FM. Importance of Nernst effect in electromagneto-acoustic transformation. Low Temp Phys. 1992;18:737.
31. Vasil'ev AN, Maallavi FM, Kaganov MI. Thermoelastic stresses as a mechanism of electromagnetic-acoustic transformation. Soviet Physics Uspekhi. 1993;36:968.
32. Krstovska D, Galbova O, Sandev T. Thermoelectric mechanism of electromagnetic-acoustic transformation in organic conductors. Europhys Lett. 2008;81:37006.
33. Krstovska, D. Ultrasonic wave generation in two-band organic conductors due to thermoelectric effect. Int J Mod Phys B. 2017;31: *(In press)*.
34. Abrikosov AA. Fundametals of the theory of metals. 2nd ed. North-Holland: Amsterdam; 1988.
35. Kovalev AE, Hill S, Qualls JS. Determination of the fermi velocity by angle-dependent periodic orbit resonance measurements in the organic conductor α-$(BEDT\text{-}TTF)_2KHg(SCN)_4$. Phys Rev B. 2002;66:134513.